NANO LETTERS

2004
Vol. 4, No. 2
327−330

Synthesis and Optical Properties of "Branched" Gold Nanocrystals

Encai Hao, Ryan C. Bailey, George C. Schatz,* Joseph T. Hupp,* and Shuyou Li

Department of Chemistry, Northwestern University, Evanston, Illinois 60208-3113

Received December 10, 2003; Revised Manuscript Received December 18, 2003

ABSTRACT

We report the synthesis of new "branched" gold nanocrystals in high yield (over 90%) via a wet-chemical route. The branched nanocrystals exhibit a shape-dependent plasmon resonance that is red-shifted by 130–180 nm from the spherical particle wavelength. Discrete dipole approximation (DDA) calculations qualitatively replicate the observed optical extinction spectra of the nanocrystals, indicating that the surface plasmon resonance is mainly determined by in-plane dipole excitation associated with the sharp tips.

Introduction. The synthesis of inorganic nanocrystals with controllable shapes is an important goal of modern materials chemistry. This field has been characterized by rapid progress in the past few years,[1−3] with the synthesis of rods,[1,4−7] triangular prisms,[2,8,9] disks,[10−13] cubes,[14] and even branched tetrapods[15] having been reported, often in high yield. Beyond their aesthetic appeal, these new structures are compelling for multiple fundamental and practical technological reasons. First, their synthesis has motivated experimental progress in understanding the intrinsic shape-dependent properties of metal and semiconductor nanocrystals.[1,2,5] Second, some of these structures feature optical and electrical properties that make them desirable for emerging applications including biolabels, photovoltaic behavior,[16] chemical sensing, and surface enhanced Raman scattering, among others. Third, some of these structures enable elucidation of the particle growth mechanism,[9,15,17] which in turn may make possible the prediction and systematic manipulation of the final nanocrystal structure. Finally, these new materials provide new template systems for the further generation of different structures.[18,19]

Although extensive studies, thousands of papers, have focused on gold nanoparticles, the wet chemical synthesis of nonspherical gold nanoparticles remains limited (at least in high yield) to rods,[1,4,6,7] triangular/hexagonal/sphere mixtures,[20] and cubes.[14] Herein, the synthesis and characterization of new-branched gold nanocrystals is reported. Furthermore, we have attempted to understand the shape-guided growth process, and we have briefly characterized the optical properties of the new particles experimentally and via discrete dipole approximation (DDA) electrodynamics calculations.[21,22]

Experimental Section. In a typical synthesis, 4 mg of bis-(*p*-sulfonatophenyl) phenylphosphine dihydrate dipotassium (BSPP) and 0.2 mL of 30% H_2O_2 were added to 100 mL of 6.8×10^{-3} M sodium citrate solution. Under constant shaking, 200 μL of 0.05 M $HAuCl_4$ was added slowly at room temperature. Over several minutes, the solution color changed from colorless to blue. The resulting blue colloids can be kept for several days in a refrigerator, although eventually a spectral shift to the blue takes place, presumably indicative of particle annealing.

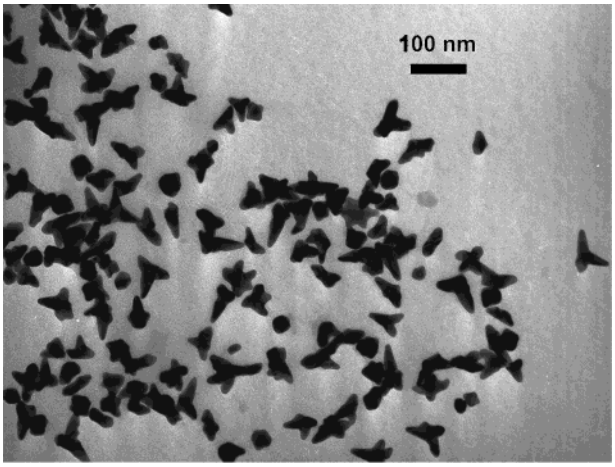

Figure 1. TEM image of branched gold nanocrystals.

Results and Discussion. The gold nanoparticles were characterized structurally with transmission electron microscopy (TEM) using a JEOL 2010F operated at an acceleration voltage of 300 kV. Figure 1 shows gold nanoparticles with one, two or three tips in over 90% yield. Among them, three-tipped nanoparticles are in the majority comprising over 50% of the total particle population. The length of the well-formed tips is roughly 30 nm, but because of the asymmetric shapes, the overall particle sizes show significant variation. It is worth mentioning that the sharp curvature of each tip is different

* Corresponding authors. E-mail: schatz@chem.northwestern.edu; jthupp@chem.northwestern.edu

10.1021/nl0351542 CCC: $27.50
Published on Web 01/09/2004

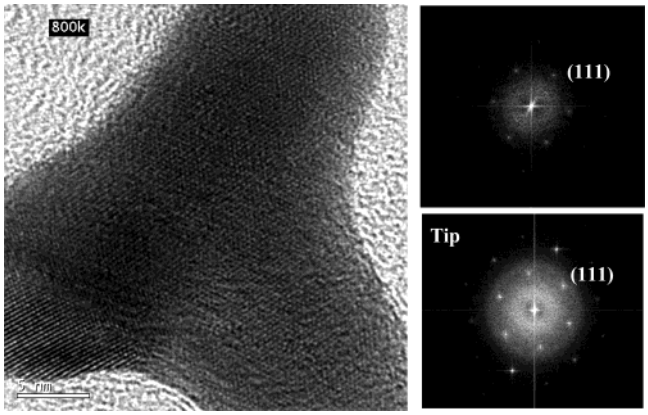

Figure 2. High-resolution TEM images of an individual gold nanocrystal. Right panels show Fourier transformation pattern of the whole image (upper) and tip region (bottom).

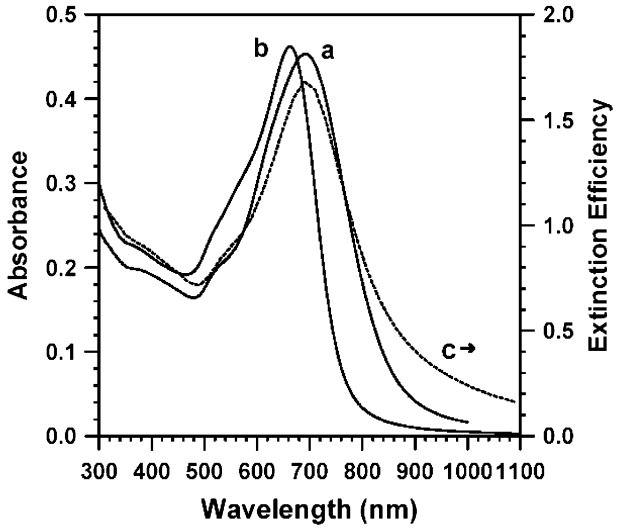

Figure 3. UV−visible spectra of branched gold nanocrystals obtained using different concentrations of BSPP (denoted (a) and (b)). The dashed line denoted (c) shows the calculated extinction spectrum using the DDA method.

from the "multipods" that have been observed recently in several systems.[15,17,23]

Figure 2 shows a high-resolution transmission electron microscope (TEM) image of an individual particle. This displays hexagonal symmetry, consistent with the {111} direction of the face-centered cubic (fcc) structure of gold. Fourier transforms (FTs) of various regions of the image reinforce the assignment of the fcc {111} direction of gold. Furthermore, comparison of FTs collected separately for the particle center region and tip region are nearly identical, confirming that the branched Au particles are composed of a single crystal.

In contrast to the characteristic red color of spherical Au nanoparticles, the colloidal solution of the branched Au nanocrystals is blue. The measured extinction spectrum is shown in Figure 3 and it shows a plasmon resonance peak that is red-shifted from ca. 500−530 nm for spheres to 690 nm for the branched particles. The plasmon band can be varied in the range from 650 to 700 nm, depending on the reactant and surfactant concentration. Figure 3 shows that

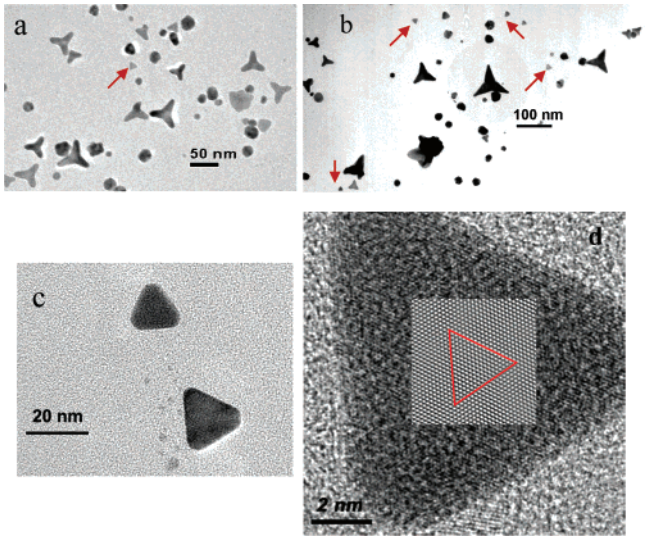

Figure 4. (a) and (b) TEM images of gold nanocrystals that were synthesized without BSPP during the initial particle growth; (c) an enlarged image of tiny triangular nuclei; and (d) the high-resolution images of individual triangular nuclei, where the center area is filtered pattern according to the {111} direction of fcc structure of gold. Arrows show small triangular prisms that are discussed in the text.

doubling the BSPP concentration (i.e., adding 7.5 mg in the synthesis) leads to a narrower plasmon band that is centered at 657 nm. TEM results show that both samples are branched Au nanocrystals, however, the samples with the plasmon band at 657 nm have smaller average sizes. From a practical standpoint, the shape dependent optical properties of reactive gold colloids represent convenient experimental reporters in studies of crystal growth.

Remarkably, thin trigonal gold platelets, but of micron size and lacking distinct tips, were reported more than a half-century ago.[24,25] The micron-sized particles (1−3 μm) were obtained via the reduction of chloroauric acid by hydrogen peroxide at elevated temperatures. Usually, this reduction by either citrate or hydrogen peroxide is slow at room temperature. To our surprise, the reaction is substantially accelerated when both are employed, as shown by the formation of the blue Au colloids within several minutes. As a result, it is difficult to elucidate the kinetic processes underlying particle growth. To date, the standard explanation for anisotropic particle growth in liquid media involves the use of appropriate capping reagents to kinetically control the growth rate of various facets of a seed.[5,11,15] In our experiments, synthesis[26] without BSPP during initial growth produces only symmetrical "three-tipped" Au nanocrystals, indicating that the role of BSPP is not essential for formation of the branched structures. As shown in Figures 4a and 4b, the overall yield of "three-tipped" Au nanocrystals (grown without BSPP) can be as high as 40−50%, and the average tip to tip distance in the nanocrystals is 42 nm. Tiny triangular prisms (10 nm edge length) are also found in the same batch, each comprising a single-crystal having an orientation identical to that of the larger "three-tipped" Au nanocrystals. We speculate that the tiny triangular prisms function as early-stage nuclei for "three-tipped" particle formation and growth.

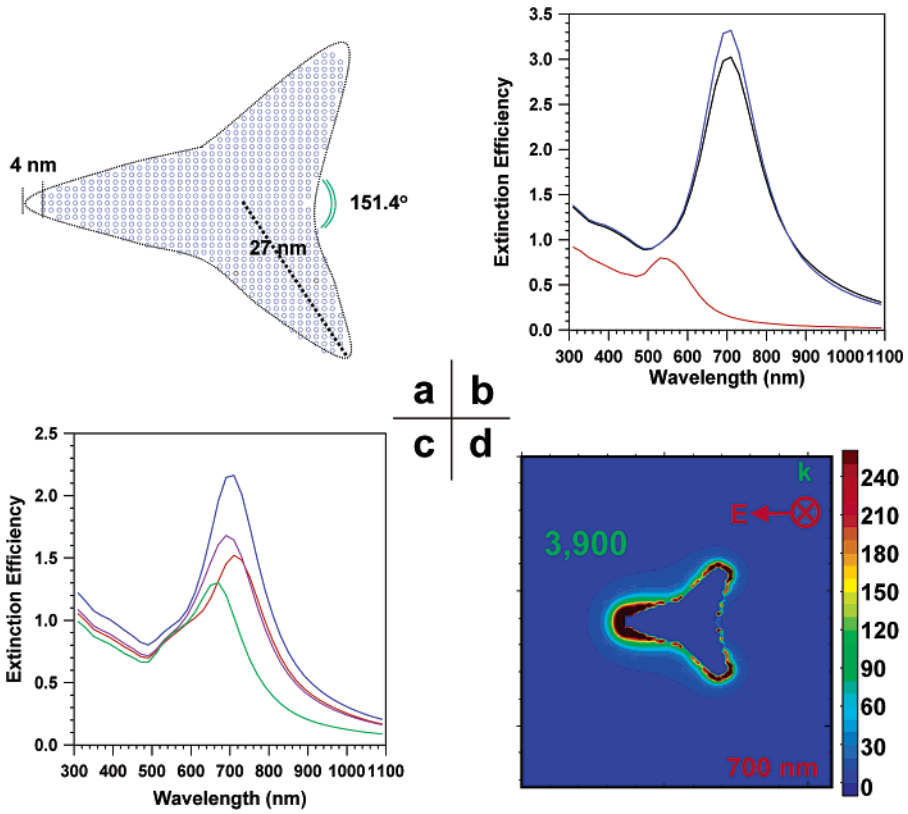

Figure 5. (a) Schematic representation of a symmetrical three-tipped Au nanocrystal that is used in the DDA calculations, showing the outline of the particle before snipping, and the DDA grid after snipping. (b) Calculated extinction spectra of a single gold nanocrystal for two in-plane polarization directions and one out-of-plane direction. (c) The calculated spectra of gold nanocrystals including one-tipped (green), two-tipped (red), asymmetric three-tipped (purple), and symmetric three-tipped particles (blue). (d) E-field enhancement contours external to a symmetrical three-tipped gold nanocrystal for polarization along one tip and with the wavelength taken to be the plasmon peak at 700 nm. The peak value of $|E|^2$ at the particle tip is 3900 times the applied field.

To get the "three-tipped" particles, the growth has to be fastest perpendicular to the edge of the triangle, i.e., parallel to the {200} direction and perpendicular to the {111} direction.[24] Presumably the role of BSPP is to influence the growth rates of certain crystal facets of the seeds, leading to the formation of the anisotropic branched structures in Figure 1.

Electromagnetic Simulations. To understand the measured optical features in Figure 3, we have solved Maxwell's equations for light interacting with a 14 nm thick "three-tipped" gold nanocrystal featuring 48 nm tip-to-tip distances and 4 nm snipping (meaning that, analogous to earlier work,[21] a 4 nm region at the tips is removed in order to mimic the expected annealing of the sharpest features). This yields a particle with a 42 nm tip-to-tip distance, which matches the average value observed in Figure 4. Figure 5a shows the resulting structure for the case where we have chosen to make three identical tips. We have also studied asymmetrical structures with a long tip and two short tips, as well as structures with only one or two tips. The electrodynamics calculations were done using a finite element-based method known as the discrete dipole approximation (DDA),[21,22] which has proven particularly useful for describing isolated nanoparticles of arbitrary shape in arbitrarily defined surrounding environments.[2,21] In the DDA, the object of interest is represented as a cubic array of N polarizable elements (which is schematically indicated in Figure 5a). The response of this array to an applied electromagnetic field is then described by self-consistently determining the induced dipole moment within each element. The spatially resolved dipole information can then be used to determine key optical properties such as the extinction efficiency and the electromagnetic field (E-fields) near the particle surface.[27] Local E-field enhancements, associated with surface plasmon excitation, are major contributors to surface-enhanced Raman scattering.[21,28]

As shown in Figure 5b, two absorption bands (700 and 540 nm) are found in the computations for the symmetrical three-tipped particle. Examination of the induced polarizations associated with these spectral features indicates that the 700 nm peak is the in-plane dipole plasmon resonance and the 540 nm peak is the out-of-plane quadrupole resonance. The calculated orientationally averaged spectrum for the isolated 14 × 48 nm symmetrical three-tip particle is shown as the dashed line in Figure 3. We find that the calculated line shape agrees qualitatively with the experimental spectrum and quantitatively with respect to the wavelength of the plasmon maximum. Further calculations indicate that the plasmon bands of the three-tipped Au nanocrystals are very sensitive to the length and the sharpness of the tips but less sensitive to the thickness and overall size of the particles.

In our experiments, we observed relatively narrow plasmon absorptions (Figure 3) from the branched Au nanocrystals.

However, the Au nanocrystals are not uniform (see Figure 1), so it is important to determine what effect this has on the extinction spectra. To do this, we have performed calculations for Au nanocrystals that have three asymmetrical tips, two tips, and even one tip. As shown in Figure 5c, we find that these nanostructures have an extinction spectrum similar to the symmetrical particle, with plasmon resonances that are centered near 695 nm. (One exception is the one-tipped particles that are blue-shifted to 674 nm.) Based on these results, it is clear that in-plane dipole excitation from the particle tips dominates the optical properties of these particles, and (fortunately) the heterogeneous shape distribution has a rather small effect on the spectrum.

Figure 5d shows contours of the calculated E-field (plotted as $|E|^2$) external to a three-tipped Au nanocrystal upon excitation at the plasmon maximum. The largest enhancements (peak fields) occur, as one might have anticipated, at the sharp tips of the particle, with enhancements being about 3900 times the applied field. The large calculated maximum field enhancements for the three-tip Au nanocrystal suggest that particles of this kind could be useful for achieving large surface Raman enhancements (E^4-dependent enhancements).[28]

Conclusion. We report the synthesis of branched gold nanocrystals in high yield via a wet-chemical route. High-resolution TEM measurements show that each gold particle is a single crystal. Tiny triangular prisms formed during the initial stages of synthesis are speculatively identified as nuclei for the branched-particle formation, which involves anisotropic growth perpendicular to the edges of the triangular prism. DDA calculations qualitatively indicate that the observed optical extinction spectra of the branched nanocrystals are mainly determined by in-plane dipole excitation associated with the tips of the particles. The calculations also indicate that large electromagnetic field enhancements exist at the particle tips, suggesting that they could be of value in applications involving surface-enhanced Raman scattering.

Acknowledgment. We gratefully acknowledge support from the National Science Foundation through the Materials Research Center (MRSEC) and the Air Force Office of Scientific Research MURI program (F49620-02-1-0381). E.H. thanks Mr. Haiping Sun (University of Michigan) for great help on the TEM measurements.

References

(1) Link, S.; El-Sayed, M. A. *J. Phys. Chem. B* **1999**, *103*, 8410.
(2) Jin, R.; Cao, Y.; Mirkin, C. A.; Kelly, K. L.; Schatz, G. C.; Zheng, J. *Science* **2001**, *294*, 1901.
(3) Callegari, A.; Tonti, D.; Chergui, M. *Nano Lett.* **2003**, *3*, 1565.
(4) Yu, Y.-Y.; Chang, S.-S.; Lee, C.-L.; Wang, C. R. C. *J. Phys. Chem. B* **1997**, *101*, 6661.
(5) Peng, X.; Manna, L.; Yang, W.; Wickham, J.; Scher, E.; Kadavanich, A.; Alivisatos, A. P. *Nature* **2000**, *404*, 59.
(6) Jana, N. R.; Gearheart, L.; Murphy, C. J. *J. Phys. Chem. B* **2003**, *105*, 4065.
(7) Kim, F.; Song, J. H.; Yang, P. *J. Am. Chem. Soc.* **2002**, *124*, 14316.
(8) Sun, Y.; Mayers, B.; Xia, Y. *Nano Lett.* **2003**, *3*, 675.
(9) Yang, J.; Fendler, J. H. *J. Phys. Chem.* **1995**, *99*, 5505.
(10) Maillard, M.; Giorgio, S.; Pileni, M.-P. *Adv. Mater.* **2002**, *14*, 1084.
(11) Puntes, V. F.; Zanchet, D.; Erdonmez, C. K.; Alivisatos, A. P. *J. Am. Chem. Soc.* **2002**, *124*, 12874.
(12) Hao, E.; Kelly, K. L.; Hupp, J. T.; Schatz, G. C. *J. Am. Chem. Soc.* **2002**, *124*, 15182.
(13) Maillard, M.; Huang, P.; Brus, L. *Nano Lett.* **2003**, *3*, 1611.
(14) Sun, Y.; Xia, Y. *Science* **2002**, *298*, 2139.
(15) Manna, L.; Milliron, D. J.; Meisel, A.; Scher, E. C.; Alivisatos, A. P. *Nature Mater.* **2003**, *2*, 382.
(16) Huynh, W. U.; Dittmer, J. J.; Alivisatos, A. P. *Science* **2002**, *295*, 2425.
(17) Lee, S.-M.; Jun, Y.-W.; Cho, S. N.; Cheon, J. *J. Am. Chem. Soc.* **2002**, *124*, 11244.
(18) Obare, S. O.; Jana, N. R.; Murphy, C. J. *Nano Lett.* **2001**, *1*, 601.
(19) Metraux, G. S.; Cao, Y. C.; Jin, R.; Mirkin, C. A. *Nano Lett.* **2003**, *3*, 519.
(20) Malikova, N.; Pastoriza-Santos, I.; Schierhorn, M.; Kotov, N. A.; Liz-Marzán, L. M. *Langmuir* **2002**, *18*, 3694.
(21) Kelly, K. L.; Coronado, E.; Zhao, L. L.; Schatz, G. C. *J. Phys. Chem. B* **2003**, *107*, 668.
(22) Yang, W.-H.; Schatz, G. C.; Van Duyne, R. P. *J. Chem. Phys.* **1995**, *103*, 869; Program DDSCAT, by BT Draine, P. J. Flatau. University of California, San Diego, Scripps Institute of Oceanography, 8605 La Jolla Dr., La Jolla, CA 92093-0221.
(23) Chen, S.; Wang, Z.; Ballato, J.; Foulger, S. H.; Carroll, D. *J. Am. Chem. Soc.* **2003**, *125*, 16186.
(24) Suito, E.; Ueda, N. *Science (Japan)* **1953**, *1951*.
(25) Milligan, W. O.; Morriss, R. H. *J. Am. Chem. Soc.* **1964**, *86*, 3461.
(26) Typically, 200 μL of 0.05 M $HAuCl_4$ and 200 μL of 30% H_2O_2 were added with stirring at room temperature to 100 mL of 6.8×10^{-3} M sodium citrate. After 10 s, the stirring was stopped. Over several minutes a series of solution colors was observed, beginning with pale yellow ($HAuCl_4$) through colorless to blue. Five minutes after the appearance of the blue color, 1 mL of BSPP solution (7.5 mM) was added dropwise as a stabilizing agent.
(27) Jensen, T.; Kelly, K. L.; Lazarides, A.; Schatz, G. C. *J. Cluster Sci.* **1999**, *10*, 295.
(28) Schatz, G. C. *Acc. Chem. Res.* **1984**, *17*, 370.

NL0351542